Wierenga, R. K., de Jong, R. J., Kalk, K. H., Hol, W. G. J., & Drenth, J. (1979) *J. Mol. Biol. 131*, 55–73.
Wierenga, R. K., Kalk, K. H., van der Laan, J. M., Drenth, J., Hofsteenge, J., Weijer, W. J., Jekel, P. A., Beintema, J. J., Müller, F., & van Berkel, W. J. H. (1982) in *Flavins and Flavoproteins* (Massey, V., & Williams, C. H., Eds.) pp 11–18, Elsevier/North-Holland, Amsterdam.
Wijnands, R. A., Weijer, W. J., Müller, F., Jekel, P. A., Van Berkel, W. J. H., & Beintema, J. J. (1986) *Biochemistry 25*, 4211–4218.

Reaction of Porcine Pancreatic Elastase with 7-Substituted 3-Alkoxy-4-chloroisocoumarins: Design of Potent Inhibitors Using the Crystal Structure of the Complex Formed with 4-Chloro-3-ethoxy-7-guanidinoisocoumarin†

James C. Powers,* Józef Oleksyszyn, S. Lakshmi Narasimhan, and Chih-Min Kam
School of Chemistry, Georgia Institute of Technology, Atlanta, Georgia 30332
R. Radhakrishnan and E. F. Meyer, Jr.*
Department of Biochemistry, Texas A&M University, College Station, Texas 77843
Received June 9, 1989; Revised Manuscript Received November 27, 1989

ABSTRACT: The crystal structure of the acyl enzyme formed upon inhibition of porcine pancreatic elastase (PPE) by 4-chloro-3-ethoxy-7-guanidinoisocoumarin has been determined at a 1.85-Å effective resolution. The chlorine atom is still present in this acyl enzyme, in contrast to the previously reported structure of the 7-amino-4-chloro-3-methoxyisocoumarin–PPE complex where the chlorine atom has been replaced by an acetoxy group. The guanidino group forms hydrogen bonds with the carbonyl group and side-chain hydroxyl group of Thr-41, and the acyl carbonyl group has been twisted out of the oxyanion hole. Molecular modeling indicates that the orientation of the initial Michaelis enzyme–inhibitor complex is quite different from that of the acyl enzyme since simple reconstruction of the isocoumarin ring would result in unfavorable interactions with Ser-195 and His-57. Molecular models were used to design a series of new 7-(alkylureido)- and 7-(alkylthioureido)-substituted derivatives of 3-alkoxy-7-amino-4-chloroisocoumarin as PPE inhibitors. All the 3-ethoxyisocoumarins were better inhibitors than those in the 3-methoxy series due to better interactions with the S_1 pocket of PPE. The best ureido inhibitor also contained a *tert*-butylureido group at the 7-position of the isocoumarin. Due to a predicted interaction with a small hydrophobic pocket on the surface of PPE, this isocoumarin and a related phenylthioureido derivative are among the best irreversible inhibitors thus far reported for PPE ($k_{obs}/[I]$ = 8100 M^{-1} s^{-1} and 12 000 M^{-1} s^{-1}). Kinetic studies of the stability of enzyme–inhibitor complexes suggest that many isocoumarins are alkylating the active site histidine at pH 7.5 via a quinone imine methide intermediate, while at pH 5.0, the predominant pathway appears to be simple formation of a stable acyl enzyme derivative.

There is considerable interest in the design of inhibitors for elastases, which are thought to play a major role in the tissue destruction associated with arthritis, pancreatitis, and pulmonary emphysema (Janoff & Dearing, 1980; Powers & Bengali, 1986). Modern methods of rational drug design utilize computer graphics to model the binding of inhibitors to the active site of the targeted enzyme and can lead to the design of new inhibitors through visualization of preferred interactions between the enzyme and inhibitors (Gund et al., 1987). These methods should be very fruitful with elastases because the crystal structures of porcine pancreatic elastase (PPE)[1] and human leukocyte elastase (HLE) have been determined at atomic resolution and are available for molecular modeling (Bode et al., 1989).

Another requirement for successful inhibitor design is an X-ray structure of a complex between the targeted enzyme and one or more members of the class of inhibitors being investigated. These structures can then serve as "leads" for further modeling, design, and synthesis. Fortunately, several enzyme–inhibitor complexes are available with the elastases, including two peptide chloromethyl ketone complexes with HLE (Wei et al., 1988; Navia et al., 1989), two peptide fluoro ketones with PPE (Takahashi et al., 1988, 1989), and two benzoxazinones with PPE (Radhakrishnan et al., 1987).

Heterocyclic compounds such as 3-alkoxy-7-amino-4-chloroisocoumarins exhibit potent inhibitory activity toward a number of serine proteases including HLE and PPE (Harper & Powers, 1985; Kam et al., 1988). Many isocoumarins simply form acyl enzymes with serine proteases as a result of nucleophilic attack of the Ser-195 hydroxyl group on the isocoumarin carbonyl group. However, some isocoumarins are mechanism-based inhibitors in which a reactive group is unmasked during the acylation reaction and subsequently reacts with other residues in the active site of the enzyme, leading to irreversible inhibition. The structure of the acyl enzyme

†Supported by grants from the National Institutes of Health to J.C.P. (HL 29307 and HL 34035) and from the Robert A. Welch Foundation (A328) and the Texas Agricultural Experiment Station to E.F.M. Computational resources were provided by Associate Provost for Computing, Dr. John Dinkel (Texas A&M).

[1] Abbreviations: CDI, 1,1′-carbonyldiimidazole; EIC, 7-amino-4-chloro-3-ethoxyisocoumarin; GIC, 4-chloro-3-ethoxy-7-guanidinoisocoumarin; Hepes, 4-(2-hydroxyethyl)-1-piperazineethanesulfonic acid; HLE, human leukocyte (neutrophil) elastase; IC, isocoumarin; MIC, 7-amino-4-chloro-3-methoxyisocoumarin; NA, *p*-nitroanilide; PPE, porcine pancreatic elastase; Suc, succinyl.

0006-2960/90/0429-3108$02.50/0

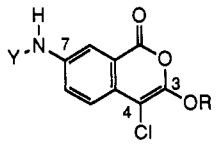

FIGURE 1: Structure of isocoumarin inhibitors of porcine pancreatic elastase. Isocoumarins where Y = H are 3-alkoxy-7-amino-4-chloroisocoumarins. For example, 7-amino-4-chloro-3-methoxyisocoumarin (MIC) has Y = H and R = CH_3; 7-amino-4-chloro-3-ethoxyisocoumarin (EIC) has Y = H and R = CH_3CH_2. The 7-guanidino-, 7-ureido-, and 7-thioureidoisocoumarins have Y = $H_2NC(=NH_2^+)$, H_2NCO (carbamoyl group), and H_2NCS (thiocarbamoyl group), respectively. For example, 4-chloro-3-ethoxy-7-guanidinoisocoumarin [$H_2NC(=NH_2^+)$-EIC] has Y = $H_2NC(=NH_2^+)$ and R = CH_3CH_2; 7-[(*tert*-butylcarbamoyl)amino]-4-chloro-3-ethoxyisocoumarin (*t*-BuHNCO-EIC) has Y = *t*-BuHNCO and R = CH_3CH_2.

formed upon inhibition of PPE with 7-amino-4-chloro-3-methoxyisocoumarin (Figure 1) has been determined to near-atomic resolution (Meyer et al., 1985).

In this paper, we report the X-ray crystallographic analysis of the acyl enzyme obtained by reaction of PPE and 4-chloro-3-ethoxy-7-guanidinoisocoumarin (Figure 1). This isocoumarin is a potent mechanism-based inhibitor of trypsin and trypsin-like enzymes (Kam et al., 1988) and also reacts readily with elastases. Comparison of the guanidinoisocoumarin structure with the 7-amino-4-chloro-3-methoxyisocoumarin–PPE structure revealed differences in the positions of both the inhibitor atoms and the active site residues. Molecular modeling was utilized to design a new series of isocoumarin inhibitors based on this crystal structure. The rates of inhibition of PPE by many of the new inhibitors are better than those observed with the parent isocoumarin, showing that molecular modeling is an effective tool in the design of new elastase inhibitors.

Materials and Methods

Porcine pancreatic elastase was obtained from Serva and Sigma Chemical Co., St. Louis, MO. Hepes was purchased from Research Organics Inc., Cleveland, OH, and Suc-Ala-Ala-Ala-NA was purchased from Peninsula Laboratories, Inc., Belmont, CA. The isocoumarins, 7-amino-4-chloro-3-methoxyisocoumarin (**1**), 7-amino-4-chloro-3-ethoxyisocoumarin (**2**; Harper & Powers, 1985), 4-chloro-7-guanidino-3-methoxyisocoumarin [$H_2NC(=NH_2^+)$-MIC], and 4-chloro-3-ethoxy-7-guanidinoisocoumarin [$H_2N(C=NH_2^+)$-EIC; Kam et al., 1988], were prepared as previously described.

X-ray Structure. PPE (Serva) was crystallized without purification. A large (0.4 × 0.4 × 0.6 mm) crystal was mounted in a thin-walled capillary in the presence of excess solid 4-chloro-3-ethoxy-7-guanidinoisocoumarin and allowed to soak for 10 h at −1 °C. Data collection was begun by using the rotation method with a Huber flat-plate camera, a crystal to film distance of 47 mm, and a temperature of −1 °C. Photographs were taken over a 3° range and at a rotation rate of 2°/h, according to the accelerated method of Radhakrishnan et al. (1987). A 0.5-mm collimator was used. After 4 days the crystal cracked and subsequent films were not interpretable, so the crystal was discarded and a smaller (0.3 × 0.3 × 0.4 mm) crystal was soaked under similar conditions; this crystal was used to measure the remainder of the asymmetric scan range. Data from both crystals were evaluated by the program FILME [Schwager et al. (1975) with modifications by William Bennett (unpublished work)].

A total of 34 160 reflections were measured and input to the PROTEIN system of programs (Steigemann, 1974) for scaling and merging. Two film packs did not merge well and were rejected. R_{merge} measures the agreement of intensity measurements from each source with mean values obtained from several sources and is defined as $\sum|I_i - \langle I\rangle|/\sum I_i$, where I_i is the intensity value of individual measurements and $\langle I\rangle$ the corresponding mean value, the summation over all measurements common to two or more films. R_{merge} ranged from 3.67% to 11.53%. The R_{scale} values (defined as the agreement of its mean value with mean values derived from at least two sources) were evaluated for each source and ranged from 5.04% to 12.06%. The R_{merge} value for the entire data set, 8.42%, was obtained from a total of 21 661 measurements which gave 15 761 unique reflections above the 1σ level to 1.74-Å resolution. An additional 1177 unique reflections were measured to 1.65-Å resolution but were deemed to contribute too little to justify an analysis at that resolution. The data set is 67% complete to 1.74-Å resolution. The data shell from 1.78- to 1.74-Å resolution is 41% complete; the data have an effective resolution (Swanson, 1987) of 1.85 Å. Data characteristics are summarized in Table I.

Table I: Refinement of the Complex of PPE with 4-Chloro-3-ethoxy-7-guanidinoisocoumarin and Crystallographic Parameters for the Final Structure

cell constants (Å)	50.62, 58.26, 75.24
space group	$P2_12_12_1$
no. of unique reflections	15 761
resolution limits (Å); completeness (%)	7.0–1.74; 67
effective resolution[a] (Å)	1.85
final *R* factor[b]	0.17
overall temp factor (Å^2)	16.0
no. of atoms	2,004
standard deviation for bond lengths (Å)	0.015
standard deviation for bond angles (deg)	2.1
min and max cutoff temp factor (Å^2)	4.0, 50.0
min and max electron density in the final difference map (eletrons/Å^3)	−0.34, 0.34

[a] Swanson, 1987. [b] Rejection ratio 1.2.

Phases were calculated by using the coordinates of native PPE (Meyer et al., 1988a) with active site ions and all water molecules removed. A difference Fourier map clearly indicated covalent attachment (contiguous density) of the isocoumarin to the catalytic Ser-195 Oγ. Other branches from the cleaved heterocycle could be fitted into the density by using the program FRODO (Jones, 1978). The methoxy complex (terminal CH_3 group of the OCH_2CH_3 omitted) was submitted to refinement using the program EREF (Jack & Levitt, 1978; Deisenhofer et al., 1985). The *R* factor dropped from 0.33 to 0.27, and the resulting difference map contained an easily recognizable residual peak in the S_1 primary specificity pocket corresponding to the terminal CH_3 group omitted from the ethoxy moiety. This group was added and refinement was allowed to continue, ions and water molecules being added at consecutive steps as they could be assigned from residual density.

The enzyme–inhibitor complex was further refined by using the program EREF. During each refinement cycle geometric restraints were first given greater weight and then relaxed in favor of the crystallographic term. The parameters used for the refinement were essentially from Jack and Levitt (1978) except for the ester linkage at the newly formed covalent bond between the inhibitor and Ser-195, the optimum values for which were taken from Schweizer and Dunitz (1982), and the force constant for the C–O bond was given the same value as that of the C–OH bond in the EREF dictionary. The EREF amino acid library was modified in order to describe the covalent bond between the enzyme and the inhibitor as a long-range bond, analogous to a disulfide bond. In the early stages

of the refinement, temperature factors for individual atoms were refined periodically and averaged for individual residues; in the later stages, these atoms and *B* factors were allowed to vary individually.

Seventy-seven cycles of refinement were calculated, intermittently followed by temperature factor refinement and addition of new water molecules. The rejection ratio (RR) defined as 2 $(|F_{obs}| - |F_{cal}|)/(|F_{obs}| + F_{cal}|)$ was set at 1.2 to eliminate the contribution of bad reflections; the final *R* factor is 0.17 for 16 405 reflections (Table I). The standard deviations for the bond lengths and bond angles for the entire structure are 0.015 Å and 2.1°, respectively. The overall temperature factor (*B*) weighted as per electron count for the enzyme alone is 16.0 Å^2 and for the inhibitor alone is 19.2 Å^2; it is 14.3 Å^2 for Ser-195 and 11.1 Å^2 for His-57.

Full occupancy was assumed on the basis of unambiguous residual density in the initial unbiased difference map. The upper limit of the error in the model, as described by Luzatti (1952) was calculated to be 0.18 Å. The final structure comprises 2004 atoms from the enzyme complex, a calcium ion, a sulfate ion, and 172 water molecules of which 29 are found at internal, conserved locations (Meyer et al., 1988a). Diffraction data and coordinates have been deposited in the Protein Data Bank under the label 8EST.

Molecular Modeling. All computer-assisted molecular modeling was carried out on a VAX 11-780 computer using an Evans and Sutherland PS330 graphics terminal for graphics display and manipulation. The following molecular modeling software was used: Chem-X (Chemical Design Ltd., Cambridge, U.K., versions July 1986–December 1987) and PS300 FRODO (Jones, 1978; versions 6.4–6.7 licensed from Rice University, Houston, TX, with local modification; A. Karrer and A. Laczkowski, unpublished work).

Synthesis. Homophthalic acid, methyl isocyanate, ethyl isocyanate, isopropyl isocyanate, *tert*-butyl isocyanate, 1,1′-carbonyldiimidazole, bromoethanol, 2-methoxyethanol, and 2-[2-(methoxy)ethoxy]ethanol were obtained from the Aldrich Chemical Co., Milwaukee, WI. All common chemicals and solvents were reagent grade or better. The purity of each compound was checked by NMR, IR, mass spectroscopy, melting point, thin-layer chromatography (TLC) on silica gel plates, and elemental analysis, and the results were consistent with the proposed structures. The solvent system used for TLC was chloroform/methanol (9:1). The NMR spectra were recorded on either a Varian T-60 or a Bruker 360-MHZ instrument. Mass spectra were recorded on a Varian MAT 1125 spectrometer. Infrared spectra were measured on a Perkin-Elmer 299 instrument. Elemental analyses were performed by Atlantic Microlabs of Atlanta, GA. The 3-alkoxy-7-amino-4-chloroisocoumarins were prepared by cyclization of the appropriate monoalkyl nitrohomophthalate with PCl_5 followed by catalytic reduction of the nitro group (Harper & Powers, 1985). The total yields (30–40%) are based on the nitrohomophthalic acid, and the physical constants of all new structures are given (vide infra).

7-Amino-4-chloro-3-propoxyisocoumarin (**3**). Yellow needles: mp 137–138 °C; one spot on TLC, $R_f = 0.62$; mass spectrum *m/e* 253 (M^+). Anal. Calcd for $C_{12}H_{12}O_3NCl$: C, 56.76; H, 4.73; N, 5.52; Cl, 13.97. Found: C, 56.75; H, 4.80; N, 5.48; Cl, 14.06.

7-Amino-4-chloro-3-isopropoxyisocoumarin (**4**). Yellow needles: mp 120–121 °C; one spot on TLC, $R_f = 0.66$; mass spectrum *m/e* 253 (M^+). Anal. Calcd for $C_{12}H_{12}O_3NCl$: C, 56.76; H, 4.73; N, 5.52; Cl, 13.97. Found: C, 56.93; H, 4.78; N, 5.51; Cl, 13.90.

7-Amino-4-chloro-3-isobutoxyisocoumarin (**5**). Yellow solid: mp 137–139 °C; one spot on TLC, $R_f = 0.66$; mass spectrum *m/e* 267 (M^+). Anal. Calcd for $C_{13}H_{14}O_3NCl$: C, 58.27; H, 5.23; N, 5.23; Cl, 13.24. Found: C, 58.50; H, 5.33; N, 5.25; Cl, 13.09.

7-Amino-3-(2-bromoethoxy)-4-chloroisocoumarin (**6**). Yellow solid: mp 134–137 °C; one spot on TLC, $R_f = 0.74$; mass spectrum *m/e* 317 (M^+). Anal. Calcd for $C_{11}H_9O_3NClBr$: C, 41.44; H, 2.83; N, 4.40. Found: C, 42.11; H, 2.87; N, 4.48.

7-Amino-3-(3-bromopropoxy)-4-chloroisocoumarin (**7**). Yellow solid: mp 98–100 °C; one spot on TLC, $R_f = 0.76$; mass spectrum *m/e* 331 (M^+). Anal. Calcd for $C_{12}H_{11}O_3NClBr$: C, 43.30; H, 3.31; N, 4.21. Found: C, 43.21; H, 3.36; N, 4.19.

7-Amino-4-chloro-3-(2-methoxyethoxy)isocoumarin (**8**). Yellow solid: mp 133–135 °C; one spot on TLC, $R_f = 0.71$; mass spectrum *m/e* 269 (M^+). Anal. Calcd for $C_{12}H_{12}O_4NCl \cdot {}^3/_4H_2O$: C, 50.89; H, 4.80; N, 4.95. Found: C, 50.92; H, 4.43; N, 4.71.

7-Amino-4-chloro-3-[2-(2-methoxyethoxy)ethoxy]isocoumarin (**9**). Yellow solid: mp 100–101 °C; one spot on TLC, $R_f = 0.72$; mass spectrum *m/e* 313 (M^+). Anal. Calcd for $C_{14}H_{16}O_5NCl$: C, 53.60; H, 5.14: N, 4.46. Found: C, 53.68; H, 5.14; N, 4.38.

N-Substituted Urea and Thiourea Derivatives of 3-Alkoxy-7-amino-4-chloroisocoumarins. All urea and thiourea derivatives of 7-amino-4-chloro-3-methoxyisocoumarin (MIC) and 7-amino-4-chloro-3-ethoxyisocoumarin (EIC) were obtained by the reaction of MIC or EIC with the appropriate isocyanate or isothiocyanate. In a typical experiment, 3-alkoxy-7-amino-4-chloroisocoumarin (1 equiv) and isocyanate (1.5 equiv) were dissolved in THF, and the solution was kept at room temperature for a few days. The solid which precipitated was filtered and recrystallized from THF/hexane.

4-Chloro-3-methoxy-7-[(methylcarbamoyl)amino]isocoumarin (MeHNCO-MIC). Yellow solid: yield 48%; mp 225–227 °C dec; one spot on TLC, $R_f = 0.66$; mass spectrum *m/e* 282 (M^+). Anal. Calcd for $C_{12}H_{11}O_9N_2Cl$: C, 50.94; H, 3.83; N, 9.90; Cl, 12.54. Found: C, 50.93; H, 3.92; N, 9.90; Cl, 12.47.

4-Chloro-7-[(ethylcarbamoyl)amino]-3-methoxyisocoumarin (EtHNCO-MIC). Yellow solid: yield 54%; mp 212–219 °C dec; one spot on TLC, $R_f = 0.56$; mass spectrum *m/e* 296 (M^+). Anal. Calcd for $C_{13}H_{13}O_4N_2Cl$: C, 52.57; H, 4.38; N, 9.43; Cl, 11.39. Found: C, 52.77: H, 4.46; N, 9.40; Cl, 11.86.

4-Chloro-7-[(isopropylcarbamoyl)amino]-3-methoxyisocoumarin (i-PrHNCO-MIC). Yellow solid: yield 58%; mp 215–216 °C; one spot on TLC, $R_f = 0.57$; mass spectrum *m/e* 310 (M^+). Anal. Calcd for $C_{19}H_{15}N_2O_4Cl \cdot {}^1/_2THF$: C, 55.49; H, 5.49; N, 8.09; Cl, 10.24. Found: C, 55.46; H, 5.36; N, 8.15; Cl, 10.36.

7-[(tert-Butylcarbamoyl)amino]-4-chloro-3-methoxyisocoumarin (t-BuHNCO-MIC). Yellow solid: yield 41%; mp 182–183 °C; one spot on TLC, $R_f = 0.62$; mass spectrum *m/e* 324 (M^+). Anal. Calcd for $C_{15}H_{17}O_4N_2Cl$: C, 55.48; H, 5.24; N, 8.63; Cl, 10.93. Found: C, 55.52; H, 5.31; N, 8.58; Cl, 10.95.

4-Chloro-3-methoxy-7-[(phenylcarbamoyl)amino]isocoumarin (PhHNCO-MIC). Yellow solid: yield 60%; mp 203–204 °C; one spot on TLC, $R_f = 0.7$; mass spectrum *m/e* 344 (M^+). Anal. Calcd for $C_{12}H_{13}N_2O_4Cl$: C, 59.23; H, 3.80; N, 8.13; Cl, 10.28. Found: C, 59.28; H, 3.82; N, 8.11; Cl, 10.35.

4-Chloro-3-ethoxy-7-[(methylcarbamoyl)amino]isocoumarin (MeHNCO-EIC). Yellow solid: yield 42%; mp 223–225 °C dec; one spot on TLC, R_f = 0.5; mass spectrum *m/e* 296 (M^+). Anal. Calcd for $C_{13}H_{13}O_4N_2Cl$: C, 52.57; H, 4.38; N, 9.43; Cl, 11.34. Found: C, 52.80; H, 4.47; N, 9.37; Cl, 11.86.

4-Chloro-3-ethoxy-7-[(ethylcarbamoyl)amino]isocoumarin (EtHNCO-EIC). Yellow solid: yield 47%; mp 215–217 °C dec; one spot on TLC, R_f = 0.58; mass spectrum *m/e* 310 (M^+). Anal. Calcd for $C_{14}H_{15}O_4N_2Cl$: C, 54.06; H, 4.83; N, 9.01; Cl, 11.41. Found: C, 54.14; H, 4.88; N, 8.98; Cl, 11.46.

4-Chloro-3-ethoxy-7-[(isopropylcarbamoyl)amino]isocoumarin (i-PrHNCO-EIC). Yellow solid: yield 52%, mp 196–198 °C; one spot on TLC, R_f = 0.54; mass spectrum *m/e* 324 (M^+). Anal. Calcd for $C_{15}H_{17}O_4N_2Cl$: C, 55.98; H, 5.24; N, 8.63; Cl, 10.93. Found: C, 55.45; H, 5.31; N, 8.58; Cl, 10.86.

7-[(tert-Butylcarbamoyl)amino]-4-chloro-3-ethoxyisocoumarin (t-BuHNCO-EIC). Yellow solid: yield 43%; mp 200–202 °C dec; one spot on TLC, R_f = 0.79; mass spectrum *m/e* 338 (M^+). Anal. Calcd for $C_{16}H_{19}O_4N_2Cl$: C, 56.66; H, 5.61; N, 8.26; Cl, 10.47. Found: C, 56.78; H, 5.66; N, 8.23; Cl, 10.51.

4-Chloro-3-ethoxy-7-[(phenylcarbamoyl)amino]isocoumarin (PhHNCO-EIC). Yellow solid: yield 65%; mp 241–242 °C dec; one spot on TLC, R_f = 0.8; mass spectrum *m/e* 358 (M^+). Anal. Calcd for $C_{18}H_{15}O_4N_2Cl$: C, 60.26; H, 4.18; N, 7.80, Cl, 9.88. Found: C, 60.45; H, 4.29; N, 7.76; Cl, 9.76.

4-Chloro-3-ethoxy-7-[(ethylthiocarbamoyl)amino]isocoumarin (EtHNCS-EIC). Yellow solid: yield 42%; mp 177–178 °C; one spot on TLC, R_f = 0.6; mass spectrum *m/e* 326 (M^+). Anal. Calcd for $C_{14}H_{15}N_2O_3ClS$: C, 51.40; H, 4.59. Found: C, 51.66; H, 4.66.

4-Chloro-3-ethoxy-7-[(phenylthiocarbamoyl)amino]isocoumarin (PhHNCS-EIC). Yellow solid: yield 55%; mp 176–177 °C dec; one spot on TLC, R_f = 0.76; mass spectrum *m/e* 341 (M^+ – SH). Anal. Calcd for $C_{18}H_{15}N_2O_3ClS$: C, 57.62; H, 4.00. Found: C, 57.77; H, 4.04.

7-(Acetylamino)-4-chloro-3-methoxyisocoumarin (MeCO-MIC). A solution containing 700 mg of 7-amino-4-chloro-3-methoxyisocoumarin in 15 mL of dry THF was treated with 2 mL of Ac_2O and 5 mg of 4-(dimethylamino)pyridine. In 5 min crystals started to precipitate. After 3 h, the solution was concentrated to about 5 mL and filtered to give 680 mg (82%): mp 210–212 °C dec; one spot on TLC, R_f = 0.76; mass spectrum *m/e* 267 (M^+). Anal. Calcd for $C_{12}H_{10}NO_4Cl$: C, 53.85; H, 3.77; N, 5.23; Cl, 13.24. Found: C, 53.84; H, 3.79; N, 5.18; Cl, 13.29.

7-(Acetylamino)-4-chloro-3-ethoxyisocoumarin (MeCO-EIC). This compound was prepared in the same manner as MeCO-MIC. Reaction of 240 mg of 7-amino-4-chloro-3-ethoxyisocoumarin and 1 mL of Ac_2O gave 140 mg (56%) of product as pale yellow crystals: mp 171–173 °C; one spot on TLC, R_f = 0.82; mass spectrum *m/e* 281 (M^+). Anal. Calcd for $C_{13}H_{12}O_4NCl$: C, 55.38; H, 4.26. Found: C, 55.49; H, 4.30.

7-(Carbamoylamino)-4-chloro-3-ethoxyisocoumarin (H_2NCO-EIC). A solution of 0.24 g of 7-amino-4-chloro-3-ethoxyisocoumarin and 0.18 g of CDI in 5 mL of THF was stirred overnight. A mixture of 5 mL of concentrated ammonia solution in water and 10 mL of water was added followed by 20 mL of THF and 20 mL of benzene. The reaction mixture was stirred for 15 min, and the organic layer was separated, washed with water, 10% citric acid, and water, and dried over magnesium sulfate. After filtration and evaporation the residue was crystallized from THF/hexane three times, giving a trace of product as yellow crystals: mp 210–212 °C dec; one spot on TLC, R_f = 0.55; mass spectrum *m/e* 282 (M^+). Anal. Calcd for $C_{12}H_{11}O_4N_2Cl$·0.25THF: C, 51.38; H, 4.32. Found: C, 51.84; H, 4.03.

7-(Carbamoylamino)-4-chloro-3-methoxyisocoumarin (H_2NCO-MIC). This compound was synthesized in the same manner from 0.22 g of 7-amino-4-chloro-3-methoxyisocoumarin and 0.18 g of CDI. A trace of product in the form of yellow crystals was obtained: mp 184–186 °C dec; one spot on TLC, R_f = 0.45; mass spectrum *m/e* 268 (M^+). Anal. Calcd for $C_{11}H_9N_2O_4Cl$: C, 49.17; H, 3.35; N, 10.43. Found: C, 48.91; H, 3.48; N, 10.19.

4-Chloro-7-[(ethoxycarbonyl)amino]-3-methoxyisocoumarin (EtOCO-MIC). A solution of 300 mg (1.33 mmol) of 7-amino-4-chloro-3-methoxyisocoumarin in 30 mL of dry THF was treated with 432 mg (4.0 mmol) of ethyl chloroformate and 202 mg (2.0 mmol) of triethylamine. The reaction mixture was left for 3 days at room temperature, then the solvent was evaporated, and the dry residue was treated with a solution of 400 mg of K_2CO_3 in 5 mL of H_2O and extracted with 20 mL of chloroform. The chloroform extract was dried with Na_2SO_4 and concentrated to about 2 mL, giving 83 mg (21%) of red crystals: mp 154–157 °C dec; one spot on TLC, R_f = 0.72; mass spectrum *m/e* 237 (M^+). Anal. Calcd for $C_{13}H_{12}ClNO_5$: C, 52.45; H, 4.06; N, 4.70; Cl, 11.91. Found: C, 52.34; H, 4.09; N, 4.68; Cl, 11.86.

4-Chloro-7-[(ethoxycarbonyl)amino]-3-ethoxyisocoumarin (EtOCO-EIC). This compound was synthesized in the same manner from 7-amino-4-chloro-3-ethoxyisocoumarin in 45% yield: mp 171–172 °C; one spot on TLC, R_f = 0.84; mass spectrum *m/e* 311 (M^+). Anal. Calcd for $C_{14}H_{14}ClNO_5$: C, 53.88; H, 4.49; N, 4.49; Cl, 11.37. Found: C, 54.00; H, 4.53; N, 4.49; Cl, 11.35.

Enzyme Inactivation–Incubation Method. Inactivation was initiated by adding a 50-μL aliquot of inhibitor in Me_2SO to 0.5 mL of a buffered enzyme solution (1.5–2.0 μM) such that the final Me_2SO concentration was 8.3% v/v at 25 °C. Aliquots (50 μL) were removed at intevals and added to a substrate solution (42-fold dilution), and the residual activity was measured spectrometrically. A 0.1 M Hepes and 0.5 M NaCl, pH 7.5, buffer was utilized throughout, and inhibitor concentrations are shown in the appropriate table. All spectrometric measurements were carried out on a Beckman Model 35 or Varian DMS-90 spectrometer. PP elastase was assayed with Suc-Ala-Ala-Ala-NA (0.714 mM; Bieth et al., 1974) and peptide 4-nitroanilide hydrolysis was measured at 410 nm (ϵ_{410} = 8800 M^{-1} cm^{-1}; Erlanger et al., 1961). First-order inactivation rate constants (k_{obs}) were obtained from plots of ln (v_t/v_0) vs time, and the correlation coefficients were greater than 0.98. Inactivation rate constants shown in the tables are typically the average of duplicate or triplicate experiments. The inhibition rates for those isocoumarins that were used at low inhibitor concentrations were also calculated according to the second-order rate law and did not differ significantly from the values obtained by using pseudo-first-order kinetics.

Deacylation Kinetics. Deacylation rates of inactivated enzymes were measured after the removal of excess inhibitor from the solution by centrifugation twice at 0 °C for 1 h using Amicon Centricon-10 microconcentrators after addition of fresh buffer. The enzymatic activity of the solution was assayed at various time intervals as described above. The first-order deacylation rates (k_{deacyl}) were obtained from plots

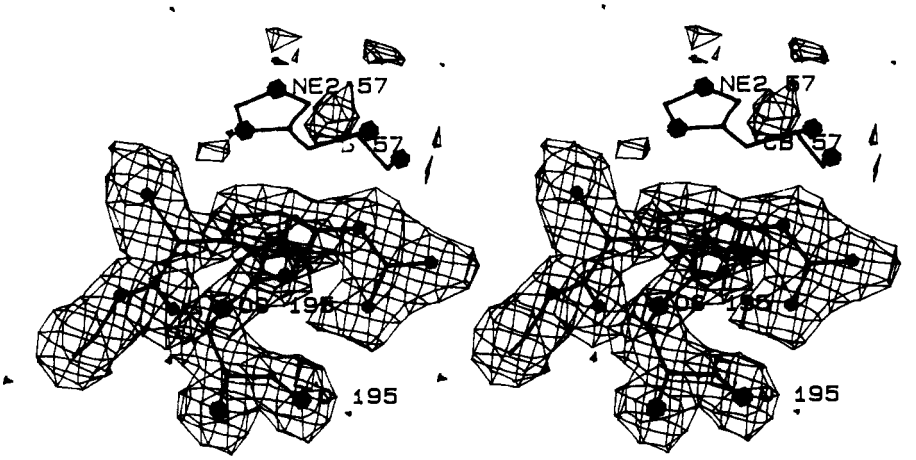

FIGURE 2: Final difference Fourier ($F_o - F_c$) map with the final model of the inhibitor superimposed.

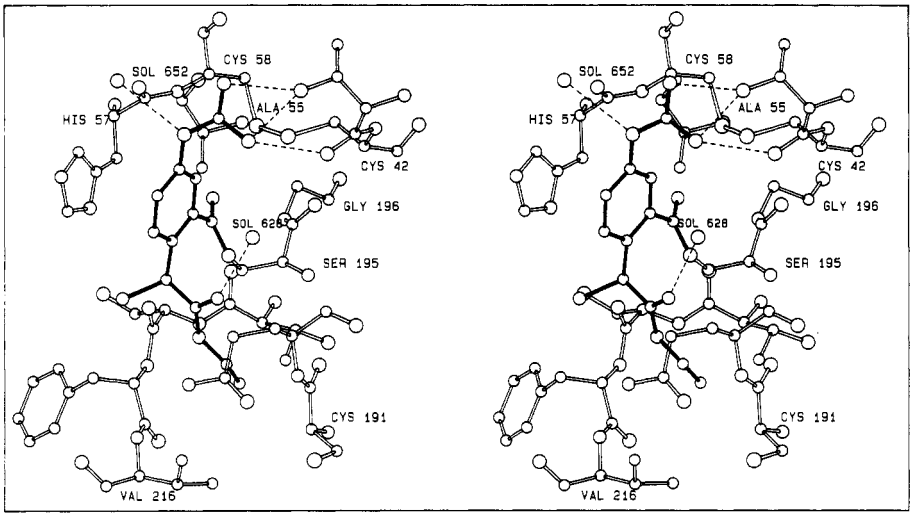

FIGURE 3: Stereoview of the complex formed upon inhibition of porcine pancreatic elastase by 4-chloro-3-ethoxy-7-guanidinoisocoumarin at pH 5.0. Hydrogen bonds are represented by dashed lines. The figure was obtained by using the computer program BALL_STICK written by one of the authors (R. Radhakrishnan, unpublished work).

of ln ($v_0 - v_t$) vs time, where v_0 is the enzyme-catalyzed substrate hydrolysis rate of the solution under the same conditions in the absence of inhibitor. The correlation coefficients were greater than 0.98.

RESULTS

X-ray Structure of the Complex of PPE and 4-Chloro-3-ethoxy-7-guanidinoisocoumarin. With Ser-195 and His-57 removed for phase calculations, the initial, unbiased Fourier difference map of the PPE–inhibitor complex immediately showed the presence of residual density in the active site, with contiguous density to Ser-195 Oγ. The imidazole ring of His-57 was rotated into the "out" position in common with previous benzoxazinone (Radhakrishnan et al., 1987) and 7-aminoisocoumarin structures with PPE (Meyer et al., 1985). A model of the 7-guanidinoisocoumarin complex was created by using the program FRODO and subjected to refinement. In the refined model (Figure 2), the ligand fits tightly into the active site of the enzyme, with the ethoxy group residing in the S_1 pocket and the guanidinium group H bonded to Thr-41 and water. The H bonds are shown in Figure 3 and listed in Table II. The oxyanion hole is partially occupied by the isocoumarin benzoyl ester carbonyl O atom. While the carbonyl group is too far (4.02 and 4.62 Å, respectively) to form H bonds to the >NH groups of Gly-193 and Ser-195, it does preempt the oxyanion hole from containing water molecules as confirmed by difference Fourier with the relevant groups removed. His-57 is in the "out" position and floats at the van der Waals surface (Figure 4) of the complex, parallel to the phenyl ring of the inhibitor. Besides the covalent attachment, this novel binding geometry is determined primarily by the S_2' interaction of Thr-41 with the guanidinium group, the interaction of the S_1 site with the ethoxy group, several H bonds, and typical van der Waals interactions (Figure 4).

Table II: Hydrogen Bonds Formed between PPE and the Inhibitor in the Acyl Enzyme Complex

donor atom	acceptor atom	distance (Å)	angle at the hydrogen (deg)
GIC N3	Thr-41 O	2.86	122
GIC N3	Thr-41 Oγ	2.91	164
GIC N2	Thr-41 Oγ	2.90	147
GIC N1	SOL 652 OH	3.16	164
SOL 628 OH	GIC 269 O2	2.90	180

Modeling of Initial PPE–Isocoumarin Complexes. In order to provide tools for the design of more effective inhibitors, models of initial Michaelis PPE–isocoumarin complexes were constructed starting from both the 4-chloro-3-ethoxy-7-guanidinoisocoumarin and 7-amino-4-chloro-3-methoxyisocoumarin acyl enzyme crystal structures. In each case, the isocoumarin ring was re-formed from the acyl enzyme structure, and then the isocoumarin was moved slightly to establish a 2.0–2.1-Å distance between Ser-195 Oγ and the carbonyl carbon atom of the inhibitor and a ca. 3-Å distance between the inhibitor carbonyl oxygen atom and the N-193 and N-195

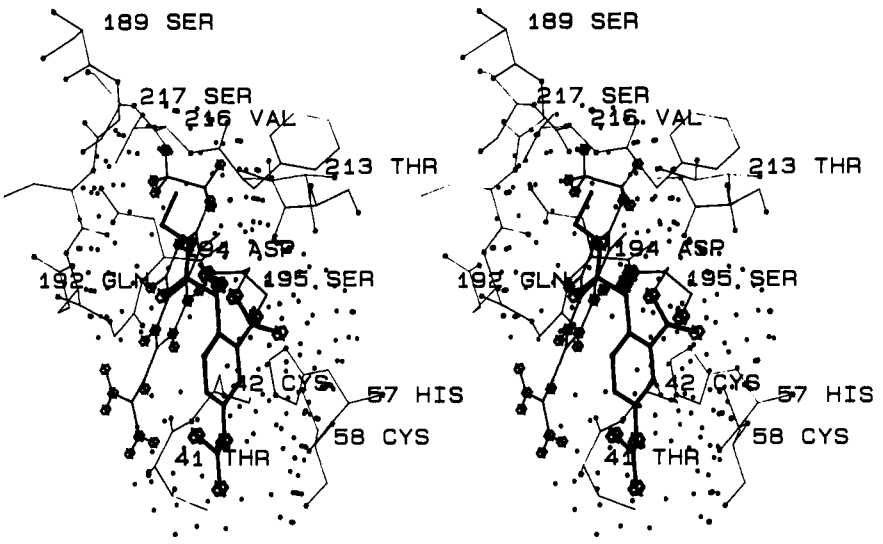

FIGURE 4: Stereoview of the active site of PPE (thin lines) containing a model of the Michaelis complex of the intact isocoumarin molecule (medium lines) and the final, refined position of the title complex (heavy lines). Heteroatoms are identified by the BLOB routine (A. Karrer, unpublished work), which has been submitted for inclusion into program FRODO (Jones, 1978). The intact isocoumarin also has H atoms drawn as BLOBS. The dotted INTERACTION surface between the inhibitor and the active site of PPE is drawn to represent the double van der Waals surface at all points less than 2 Å from protein atoms. His-57, for example, is seen thereby to make a good van der Waals contact with the inhibitor in its "out" position.

of the enzyme (oxyanion hole). The 2.0–2.1-Å distances are midway between 1.4 Å (C–O bond length) and 2.7 Å, which is the distance between Ser-195 Oγ and the carbonyl carbon atom of the P_1–P_1' bond[2] in elastase–peptide complexes (Bode et al., 1986; Meyer et al., 1988b).

The Michaelis complex of PPE with 7-amino-4-chloro-3-methoxyisocoumarin was easily constructed by re-forming the isocoumarin ring and making minor adjustments to the position of the inhibitor. In this model, the isocoumarin ring does not interfere with the Ser-195 Oγ and His-57 Nε hydrogen bond, the carbonyl oxygen atom of the isocoumarin inhibitor is located in the oxyanion hole, and the Ser-195 Oγ is positioned so that the O–C–Oγ angle is 115.5°. This geometry is nearly ideal (109°) for the nucleophilic attack of the Ser-195 Oγ on the isocoumarin carbonyl group (Dunitz, 1979). The 3-methoxy group fits into the S_1 pocket, which is consistent with previous kinetic data on the specificity of isocoumarin inhibitors (Harper & Powers, 1985).

Re-forming the isocoumarin ring in the 4-chloro-3-ethoxy-7-guanidinoisocoumarin acyl enzyme structure resulted in the insertion of the isocoumarin heterocyclic ring between Ser-195 Oγ and the imidazole ring of His-57 of PPE. This model of the Michaelis complex is unlikely since it implies that acylation of the enzyme occurs without participation of the complete catalytic triad and does not involve interaction with the oxyanion hole. A more reasonable model for the 7-guanidinoisocoumarin–PPE complex was constructed by overlapping the 7-guanidinoisocoumarin ring atoms with the corresponding atoms in the model of the 7-amino-4-chloro-3-methoxyisocoumarin Michaelis complex. In this second model (Figure 4), the 3-ethoxy group of 4-chloro-3-ethoxy-7-guanidinoisocoumarin fits into the S_1 pocket of PPE and the terminal nitrogen atoms of the 7-guanidino group are within hydrogen-bonding distance of the CO of Thr-41 and a water molecule (HOH-571) which can also form a hydrogen bond with Thr-41 Oγ. Since the catalytic triad is undisturbed and the isocoumarin carbonyl oxygen atom can interact with the oxyanion hole during acylation, this is a much more believable model for the Michaelis complex.

Formation of the 7-guanidino acyl enzyme structure as observed in the crystal structure from this model of the Michaelis complex must involve subsequent movement of the inhibitor molecule in the active site of PPE (Figure 4). We postulate that interaction between the positively charged guanidino group of the inhibitor with the favorably oriented dipoles of the Thr-41 carbonyl and hydroxyl groups could cause this movement. This would result in displacement of the Ser-195 Cβ and Oγ atoms from their positions in the native PPE structure and would also cause a change in the position of the imidazole side chain of His-57, which otherwise would make unfavorable steric contact with the inhibitor.

Inhibitor Modeling. The acyl enzyme crystal structure and the Michaelis complex model were then utilized in the design of new inhibitor structures. Examination of both models suggested that replacement of one of the nitrogen atoms of the 7-guanidino group with an alkyl group would result in favorable van der Waals interactions with the side chains of Thr-41, Tyr-35, Val-61, Arg-63 or Leu-143, and Leu-151. Since 7-guanidinoisocoumarins are difficult to synthesize, we decided instead to model the corresponding 7-ureido derivatives which can be synthesized more readily. Models of various 7-(alkylureido)-4-chloro-3-ethoxyisocoumarins complexed to PPE were constructed by using the 7-guanidinoisocoumarin Michaelis complex model, and then the exchange repulsion, dispersion, and electrostatic interactions were explored by using CHEM-X. All of the 7-(alkylureido)isocoumarins were found to have energically more favorable interactions with PPE than the parent 7-amino and 7-guanidinoisocoumarins. For the various alkyl groups studied, the order of interaction energy was *tert*-butyl < isopropyl < ethyl. The 7-(phenylureido)-isocoumarin, while being better than the 7-guanidinoisocoumarin, was not as favorable as the alkylureido derivatives. It was also apparent from the modeling that the *tert*-butyl, isopropyl, and ethyl groups could interact with either of two small hydrophobic pockets composed of the side chains of Gln-192, Leu-151, and Leu-143 or portions of the side chains of Thr-41, Tyr-35, Cys-58, Leu-63, and Phe-65. The 7-

[2] The nomenclature of Schechter and Berger (1967) is used to designate the individual amino acid residues (P_2, P_1, P_1', P_2', etc.) of a peptide substrate and the corresponding subsites (S_2, S_1, S_1', S_2', etc.) of the enzyme. The scissile bond is the P_1–P_1' peptide bond.

Table III: Rates of Inactivation of Porcine Pancreatic Elastase by 3-Alkoxy-7-amino-4-chloroisocoumarins[a]

inhibitor			$k_{obs}/[I]$
compd no.	compd name	[I] (μM)	(M^{-1} s^{-1})
1	7-amino-4-chloro-3-methoxy-IC	28–69	1500
2	7-amino-4-chloro-3-ethoxy-IC	22–76	1300
3	7-amino-4-chloro-3-propoxy-IC	73–135	500
4	7-amino-4-chloro-3-isopropoxy-IC	79	20
5	7-amino-4-chloro-3-isobutoxy-IC	105	170
6	7-amino-3-(2-bromoethoxy)-4-chloro-IC	33	1000
7	7-amino-3-(3-bromopropoxy)-4-chloro-IC	37	10
8	7-amino-4-chloro-3-(2-methoxyethoxy)-IC	230	4.3
9	7-amino-4-chloro-3-[2-(2-methoxyethoxy)ethoxy-IC	710	0.5

[a] Conditions were as follows: 0.1 M Hepes, 0.5 M NaCl, and 8.3% Me_2SO, pH 7.5 at 25 °C. Rate constants were measured as described under Materials and Methods. IC = isocoumarin.

Table IV: Inactivation Rates for Inhibition of Porcine Pancreatic Elastase by Derivatives of 7-Amino-4-chloro-3-methoxyisocoumarins MIC[a]

inhibitor	[I] (μM)	$k_{obs}/[I]$ (M^{-1} s^{-1})
$H_2NC(=NH_2^+)$-MIC	8.4	860
H_2NCO-MIC	8.2	2100
MeCO-MIC	8.3	2300
MeHNCO-MIC	13	1300
EtHNCO-MIC	6.3	1700
i-PrHNCO-MIC	12	2300
t-BuHNCO-MIC	13	3200
PhHNCO-MIC	29–46	2600
EtOCO-MIC	8.2	2000

[a] Conditions were as follows: 0.1 M Hepes, 0.5 M NaCl, and 8.3% Me_2SO, pH 7.5 at 25 °C. Rate constants were obtained as described under Materials and Methods.

(phenylureido) derivative appears to prefer the latter.

The 7-(alkylureido)- and 7-(arylureido)isocoumarins were also modeled with the 7-guanidino acyl enzyme structure as the starting point. Once again the alkyl and aryl groups of the 7-ureido substituent fit nicely into a small hydrophobic pocket composed of portions of the side chains of Tyr-35, Cys-58, Arg-61, Leu-63, and Phe-65. Visual inspection indicated that *tert*-butyl and phenylureido derivatives would fit better than the smaller isopropyl and ethyl groups. Hence, we decided to synthesize a series of 7-ureido-substituted isocoumarins and a series of isocoumarins with varying 3-alkoxy substituents to confirm the modeling predictions.

Inactivation Kinetics. Three sets of isocoumarin derivatives including 3-alkoxy-7-amino-4-chloroisocoumarins, and acyl, carbamyl, thiocarbamyl, guanidino, and urethane derivatives of both 7-amino-4-chloro-3-methoxyisocoumarin and 7-amino-4-chloro-3-ethoxyisocoumarin, were synthesized and tested as inhibitors of PPE.

The second-order inactivation rate constants ($k_{obs}/[I]$) for reaction of PPE with 3-alkoxy-7-amino-4-chloroisocoumarins are reported in Table III. The pseudo-first-order inactivation plots were linear for more than 4 half-lives. In this series of inhibitors, 7-amino-4-chloro-3-ethoxyisocoumarin, 7-amino-4-chloro-3-methoxyisocoumarin, and 7-amino-3-(2-bromoethoxy)-4-chloroisocoumarins were the best inhibitors, with $k_{obs}/[I]$ values of 1000–1500 M^{-1} s^{-1}.

The second-order inactivation rate constants ($k_{obs}/[I]$) for reaction of PPE with acyl, carbamyl, thiocarbamyl, guanidino, and urethane derivatives of 7-amino-4-chloro-3-methoxyisocoumarin (MIC) and 7-amino-4-chloro-3-ethoxyisocoumarin (EIC) are reported in Tables IV and V. The inhibition

Table V: Inactivation Rates for Inhibition of Porcine Pancreatic Elastase by Derivatives of 7-Amino-4-chloro-3-ethoxyisocoumarins (EIC)[a]

inhibitor	[I] (μM)	$k_{obs}/[I]$ (M^{-1} s^{-1})
$H_2NC(=NH_2^+)$-EIC	16	2300
H_2NCO-EIC	17	2200
MeCO-EIC	16	2100
MeHNCO-EIC	12	1400
EtHNCO-EIC	10	1700
i-PrHNCO-EIC	10	4900
t-BuHNCO-EIC	10	8100
PhHNCO-EIC	11	4200
EtOCO-EIC	9.6	3500
EtNHCS-EIC	20–50	4200
PhNHCS-EIC	9–31	12000

[a] Conditions were as follows: 0.1 M Hepes, 0.5 M NaCl, and 8.3% Me_2SO, pH 7.5 at 25 °C. Rate constants were obtained as described under Materials and Methods.

Table VI: Kinetic Constants for the Inhibition of Porcine Pancreatic Elastase by Selected Isocoumarin Derivatives[a]

inhibitor	inhibitor concn range (μM)	K_I (μM)	k_3 (s^{-1})	k_3/K_I (M^{-1} s^{-1})
3	73–225	250	0.12	500
1	28–69	140	0.22	1500
PhHNCO-MIC	29–46	110	0.28	2600
EtNHCS-EIC	20–50	92	0.39	4200

[a] Conditions were as follows: 0.1 M Hepes, 0.5 M NaCl, and 8.3% Me_2SO, pH 7.5 at 25 °C. Kinetic constants were obtained by plotting $1/k_{obs}$ vs $1/[I]$ as described by Kitz and Wilson (1962).

reactions were biphasic, and the rate constants are based on the approximately 60–80% inactivation that occurred during the first 1–2 min of incubation. Further incubation occurred at a much slower rate until complete inactivation was reached. Thus, the first-order inactivation plots were linear only for ca. 1.5–2 half-lives. Exceptions were 7-PhHNCO-MIC and the two thiourea derivatives where the pseudo-first-order inactivation plots were linear for greater than 5 half-lives (total inactivation).

In general, the 3-ethoxy derivatives were more reactive toward PP elastase than the corresponding 3-methoxyisocoumarins. The difference is small with the 7-MeHNCO and 7-EtHNCO derivatives; however, it is larger in the case of the *t*-BuHNCO derivative (3200 M^{-1} s^{-1} and 8100 M^{-1} s^{-1}). Both thiourea derivatives (EtNHCS-EIC and PhNHCS-EIC, Table V) were 2–3-fold better inhibitors than the corresponding urea derivatives.

Inhibition rates for a few representative isocoumarins were measured at varying inhibitor concentrations, and K_I and k_3 values were calculated by using the procedure of Kitz and Wilson (1962). The results obtained with four inhibitors are shown in Table VI. The plots of $1/k_{obs}$ vs $1/[I]$ for **2** and PhNHCS-EIC went through the origin, and only k_3/K_I could be determined. The overall inhibition rate (k_3/K_I) for the four inhibitors in Table VI is affected both by k_3 and K_I.

Deacylation Kinetics. The inhibitor–enzyme complexes formed upon inactivation of PPE by some of the substituted isocoumarins were very stable. The enzymatic activity was assayed after removal of excess inhibitor in the PPE–inhibitor complexes by centrifugation using Centricon-10 microconcentrators. With *i*-PrHNCO-MIC, *i*-PrHNCO-EIC, *t*-BuHNCO-MIC, *t*-BuHNCO-EIC, PhHNCO-MIC, and 4-chloro-3-ethoxy-7-guanidinoisocoumarin, no enzymatic activity was recovered at pH 7.5 even after incubation for 48 h. However, 55% of the enzymatic activity was recovered from the 3-ethoxy-7-guanidinoisocoumarin–PPE complex after in-

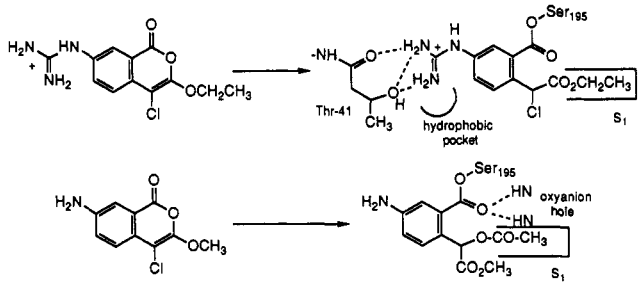

FIGURE 5: Schematic drawing of the interactions formed upon inhibition of porcine pancreatic elastase by 4-chloro-3-ethoxy-7-guanidinoisocoumarin (top) and 7-amino-4-chloro-3-methoxyisocoumarin (bottom).

cubation at pH 7.5 for 48 h. Deacylation rates for the complexes of PPE with 4-chloro-3-ethoxy-7-guanidinoisocoumarin and 3-ethoxy-7-guanidinoisocoumarin were also measured at pH 5.0 (same conditions as the X-ray experiments), and no enzymatic activity was found after 2 days. In the presence of 0.33 M hydroxylamine, 14% and 70% of the enzyme activity were recovered respectively from the PPE complexes with 4-chloro-3-ethoxy-7-guanidinoisocoumarin and 3-ethoxy-7-guanidinoisocoumarin after incubation for 2 days at pH 7.5, and ca. 40% of the enzymatic activity was recovered with both compounds after 2 days at pH 5.0.

Discussion

A variety of heterocyclic compounds have been reported as irreversible inactivators of serine proteases [reviewed in Powers and Harper (1986)]; they include 6-chloropyrones, isatoic anhydride, oxazine-2,6-diones, benzopyrone-1,4-diones, benzoxazin-4-ones, β-lactams, 3,4-dichloroisocoumarin, and 7-substituted 3-alkoxy-4-chloroisocoumains. These heterocyclic compounds react initially by acylation of the active site Ser-195 to form acyl enzymes, which may then undergo further reactions with other active site residues.

The 3-alkoxy-7-amino-4-chloroisocoumarins are mechanism-based inhibitors of elastase and other serine proteases and give rise to extremely stable inactivated enzyme complexes (Harper & Powers, 1985; Kam et al., 1988). Isocoumarins inhibit other serine proteases such as HLE much more rapidly than they react with PPE. Although the crystal structure of one PPE–isocoumarin complex is available (Meyer et al., 1985), the reasons for the low reactivity of isocoumarins with PPE and the details of the inhibition mechanism are not yet clear. Therefore, we are investigating additional crystal structures of complexes of PPE with various isocoumarins with a view to adding to the database of elastase–inhibitor complexes in order to facilitate future design work with isocoumarins and other types of heterocyclic elastase inhibitors.

X-ray Structures. 4-Chloro-3-ethoxy-7-guanidinoisocoumarin was originally designed and synthesized as an inhibitor for trypsin, thrombin, and other trypsin-like enzymes (Kam et al., 1988). The structure of the complex of this isocoumarin bound to PPE was determined since this isocoumarin readily diffused into and inhibited crystals of PPE due to the high solubility of the inactivator. Figure 5 summarizes the interactions observed in the 7-guanidinoisocoumarin complex with PPE and in the previously reported complex with 7-amino-4-chloro-3-methoxyisocoumarin (Meyer et al., 1985). Both form acyl enzymes, but otherwise the positions of the inhibitor atoms in the two acyl enzymes are quite different. The most obvious difference is the presence of the chlorine atom (*S* configuration at the benzyl carbon atom) in the 7-guanidinoisocoumarin complex. In the case of the 7-aminoisocoumarin complex, the chlorine atom has been displaced by a solvent acetoxy group (*R* configuration at the benzyl carbon atom) which occupies the S_1 pocket of the enzyme. This difference is due to a change in the buffer used to prepare the two crystalline PPE–inhibitor complexes. The 7-amino derivative was prepared in a 0.1 M acetate buffer at pH 5.0 while crystals of the 7-guanidino complex were grown and reacted in 0.1 M pH 5.0 phosphate buffer.

There are also noticeable, dramatic differences in the positions of the atoms of the aromatic ring and the 7-substituent of the inhibitor in the two complexes [see Figure 11 in Bode et al. (1989)]. The aromatic ring is bent farther away from Ser-195 in the 7-guanidino complex than in the 7-amino complex, and the two ring planes form an angle of 38.4°. The 7-amino group does not make any hydrogen bonds to PPE while the 7-guanidino group is hydrogen bonded to Thr-41 Oγ and the Thr-41 carbonyl O atom. The benzoyl carbonyl oxygen atom of the enzyme–inhibitor ester linkage is partially in the oxyanion hole in the 7-amino structure while it is out of the oxyanion hole in the complex of PPE with the 7-guanidinoisocoumarin. Because the oxyanion hole has a mechanistic role in stabilizing the intermediate oxyanion formed in both serine protease acylation and deacylation reactions, these two arrangements predict a large difference in reactivation kinetics. And finally, the positions of the catalytic Ser-195 and His-57 atoms have changed significantly from their native positions (Meyer et al., 1988a) in both the 7-guanidino structure and the 7-amino structure.

Initial PPE–Inhibitor Complex. Models of the initial noncovalent Michaelis complexes of PPE with both the 7-amino- and 7-guanidinoisocoumarins were constructed since we expected that favorable interactions between the enzyme and the inhibitor in these complexes would be reflected in an increased inhibition rate. In both models, the 3-alkoxy group of the isocoumarin inactivator is situated in the S_1 pocket of PPE. We synthesized a series of 7-aminoisocoumarins where the size of the 3-alkoxy group was systematically varied and found that the most reactive isocoumarins have 3-methoxy, 3-ethoxy, or 3-(2-bromoethoxy) substituents (Table III). The drop in inhibition rates as the size of the 3-alkoxy group is increased provides support for the Michaelis complex models since PPE is known to have a small hydrophobic S_1 pocket. The enzyme prefers the side chains of small hydrophobic residues like Ala as the P_1 residue in substrates and inhibitors.

The 3-ethoxy group of the 4-chloro-3-ethoxy-7-guanidinoisocoumarin makes better contact with the S_1 pocket of PPE than the 3-methoxy group in the 7-amino-4-chloro-3-methoxyisocoumarin Michaelis complex model, which accounts for the rather uniform increase in inhibition rate constants for the 3-ethoxy series of isocoumarins compared to the 3-methoxy inactivators (Tables IV and V). The 3-(2-bromoethoxy)isocoumarin was more reactive than expected. This is surprising since bromine is larger than a methyl group and hence this side chain is bigger than a 3-propoxy group, which results in poor inhibitory potency toward PPE. It is likely that the 3-(2-bromoethoxy)isocoumarin is exceptionally reactive due to a weak electrostatic interaction of the bromine atom with an amide bond in the active site of PPE [a crystal structure of the complex of PPE with 7-amino-3-(2-bromoethoxy)-4-chloroisocoumarin has been determined and will be reported separately].

Utilization of the X-ray Structure in Inhibitor Design. The 7-guanidinoisocoumarin acyl enzyme crystal structure and the Michaelis complex model were then used to design a series of 7-(alkylureido)-substituted 3-alkoxy-4-chloroisocoumarins, which are more potent inhibitors for PPE than the corre-

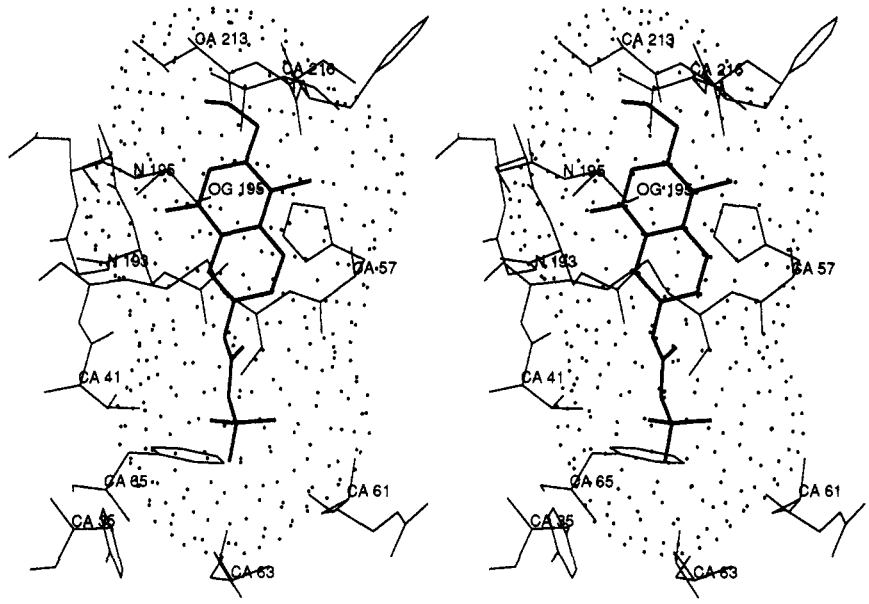

FIGURE 6: Stereoview of the proposed binding mode of 7-[(*tert*-butylcarbamoyl)amino]-4-chloro-3-ethoxyisocoumarin (*t*-BuHNCO-EIC) to the active site of PPE. The ethoxy group of the isocoumarin is placed in the S_1 pocket, and the *tert*-butyl group is shown interacting with a small hydrophobic pocket in the vicinity of Arg-61, Leu-63, Phe-65, Thr-41, and Tyr-35.

sponding 7-amino and 7-guanidinoisocoumarins. Modeling with the acyl enzyme structure suggested that adding alkyl or aryl groups to one of the nitrogen atoms of the 7-guanidino group would result in favorable van der Waals interactions with a small pocket on the surface of PPE composed of the side chains of Thr-41, Tyr-35, Cys-58, Arg-61, Leu-63, and Phe-65 (Figure 6). We also modeled the Michaelis complex and concluded that an *N*-alkyl substituent would also make favorable interactions with another nearby hydrophobic pocket composed of the side chains of Gln-192, Leu-143, and Leu-151 while an *N*-phenyl group could interact in a slightly different orientation with the same region of PPE.

To test these ideas, we chose to synthesize 7-(alkylureido)isocoumarin derivatives rather than 7-(alkylguanidino) derivatives since the former are readily synthesized by reaction of isocyanates with the corresponding 7-aminoisocoumarin. The neutral alkylureido substituent is nearly isosteric with the guanidino group and has the potential for forming the same hydrogen bonds with Thr-41 as observed in the structure of PPE with 4-chloro-3-ethoxy-7-guanidinoisocoumarin.

Isocoumarins with 7-(alkylureido) substituents are 2–8-fold more reactive with PPE than the corresponding 7-amino-4-chloro-3-methoxy- or 7-amino-4-chloro-3-ethoxyisocoumarins. As predicted from modeling, the 7-(*tert*-butylureido)-4-chloro-3-ethoxyisocoumarin was one of the best PPE inhibitors, with a $k_{obs}/[I]$ of 8100 M^{-1} s^{-1}. The isopropyl and phenyl derivatives were only half as potent but were still much better inhibitors than the other isocoumarins with shorter alkyl groups or no alkyl substituent on the ureido group. Changing the 7-guanidino group to a 7-ureido group results in almost no change in inhibition rate in the 7-ethoxyisocoumarins, indicating that all the hydrogen bonds observed in the 7-guanidinoisocoumarin acyl enzyme structure are not required for effective inhibition.

Individual kinetic parameters (K_I and k_3) were determined for several representative inhibitors (Table VI). Interestingly, the overall second-order inhibition constants (k_3/K_I) were determined by both K_I (dissociation constant of the E·I complex) and k_3 (rate of covalent bond formation from the E·I complex). The better inhibitors had both lower K_I values and higher k_3 values.

Isocoumarin Inhibitors with Urea and Thiourea Substituents. The second-order inactivation rate constants for reaction of PPE with most of the 7-ureidoisocoumarins were biphasic, which suggested the possibility that multiple forms of the inhibitor were reacting with PPE. The 7-ureidoisocoumarins contain a N,N′-disubstituted urea functional group which exists predominantly in the trans–trans form in the solid state and in solution (Mido et al. 1981) but also contains small amounts of the trans–cis and the nonplanar aut forms (Sudha & Sathyanarayana, 1984). Superposition of the trans–trans isomer of the 7-(*tert*-butylureido) derivative onto the X-ray acyl enzyme structure indicated that it would make a poor steric fit with the active site of PPE. Therefore, we believe that one of the less favorable and less abundant isomers (probably *trans*-alkyl-NHCO- and *cis*-CONH-isocoumarin) of a 7-(alkylureido)isocoumarin is actually inhibiting the enzyme during the initial rapid inactivation phase.

The stabilities of various isomers of N,N′-disubstituted thioureas are quite different from those of the corresponding ureas, and all isomers exist in more or less equal amounts (Vassilev, 1982), and thus thioureas would be predicted to react more rapidly than the ureas. Both 7-thioureido derivatives (7-EtNHCS-EIC and 7-PhNHCS-EIC) that we synthesized were 2–3 times better inhibitors than corresponding ureido derivatives, and furthermore, the pseudo-first-order inactivation plots were linear for greater than 5 half-lives. Indeed, 7-PhNHCS-EIC was the most potent inhibitor that we discovered in this research ($k_{obs}/[I]$ of 12000 M^{-1} s^{-1}).

Inhibition Mechanism. The inhibition mechanism of serine proteases by 7-substituted 4-chloro-3-alkoxyisocoumarins has been discussed previously (Harper & Powers, 1985; Kam et al., 1988) and is shown in Figure 7. The first step is acylation of Ser-195 and formation of an acyl enzyme with concurrent unmasking of the 4-aminobenzyl chloride functional group. This can eliminate chloride to give a quinone imine methide structure (center) which can react with either a solvent nucleophile or a nearby enzyme nucleophile such as His-57 to give two different acyl enzyme structures (bottom). Alternately, the chloro acyl enzyme (top right) could react directly with the nucleophiles. The acyl enzyme formed by solvolysis (bottom left) should be reactivatable by hydroxylamine, while

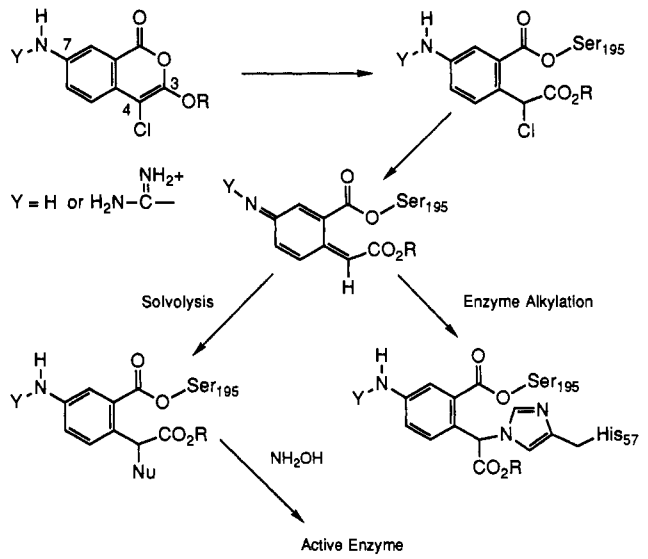

FIGURE 7: Mechanism of inhibition of porcine pancreatic elastase by 7-substituted isocoumarins.

the histidine adduct (bottom right) would be expected to be more stable.

Two intermediates in this reaction scheme have now been observed crystallographically. The complex between PP elastase and 7-amino-4-chloro-3-methoxyisocoumarin (Meyer et al., 1985) represents the acyl enzyme structure formed where the quinone imine methide reacts with a solvent nucleophile. The PPE crystals for this X-ray structure were grown and inhibited in a 0.1 M acetate buffer (pH 5.0), and as a result, the solvolysis product contains acetate. In contrast, the complex reported here represents the structure of the initial acyl enzyme where the chlorine atom is still present. In this case the conditions for crystal growth (phosphate buffer at pH 5.0) were less favorable for either solvolysis or alkylation of His-57. His-57, the only reasonable nucleophile in the vicinity of the Ser-195, would be protonated at pH 5.0 and would therefore be less likely to undergo an alkylation reaction.

Acyl Enzyme Stability. The stability of many of the PPE–isocoumarin complexes at pH 7.5 is consistent with covalent bond formation between His-57 and the inactivator. For example, PPE inactivated by 4-chloro-3-ethoxy-7-guanidinoisocoumarin or the alkylureido derivatives *i*-PrHNCO-MIC, *i*-PrHNCO-EIC, *t*-BuHNCO-MIC, *t*-BuHNCO-EIC, and PhHNCO-MIC does not regain significant activity after incubation at pH 7.5 in Hepes buffer for 2 days. Both the 4-chloro and the 7-guanidino or 7-ureido substituents are essential for this stability. At pH 7.5 the PPE complex with 4-chloro-3-ethoxy-7-guanidinoisocoumarin regained no activity after 48 h, while the complex with 3-ethoxy-7-guanidinoisocoumarin (cannot form a quinone imine methide) regained 25% activity after 24 h and a further 55% after 48 h. Addition of 0.33 M hydroxylamine had little effect on the 4-chloro-3-ethoxy-7-guanidinoisocoumarin–PPE complex (14% activity regained after 48 h) while the corresponding 7-guanidino-3-ethoxyisocoumarin–PPE complex regained 70% activity after 24 h. With the complex formed by inhibition of PPE with PhHNCO-MIC, no enzymatic activity was regained after 1 day in Hepes buffer (pH 7.5) and only 20% was recovered after treatment with 0.25 M NH_2OH for 1 day.

Our reactivation studies indicate a different reaction course at pH 5.0, the pH of the crystallographic experiment. Both 4-chloro-3-ethoxy-7-guanidinoisocoumarin and 3-ethoxy-7-guanidinoisocoumarin give stable enzyme–inhibitor complexes (no activity regained after 48 h at pH 5.0), while addition of 0.33 M hydroxylamine resulted in the recovery of 50% and 40% activity, respectively. Under these more acidic conditions (pH 5.0) hydroxylamine is a rather poor reactivating nucleophile (pK_a 7.97), and His-57 is protonated and is a poorer nucleophile in the deacylation process or as target for alkylation. Thus, at pH 5.0, the chlorine atom remains in 7-guanidinoisocoumarin–PPE crystal structure and there is no significant difference in deacylation behavior between isocoumarins with or without the 4-chloro group.

The high stability of the acyl enzymes formed from isocoumarins can also be explained without invoking covalent bond formation with His-57. Formation of an acyl enzyme from an isocoumarin–PPE Michaelis complex must result in considerable movement of various atoms in the isocoumarin structure. Modeling with the 7-guanidinoisocoumarin indicates that the electrostatic attractions between the positively charged 7-guanidino group of the inhibitor and the negative dipoles of Thr-41 carbonyl oxygen and hydroxyl oxygen atoms cause twisting of the inhibitor to form the hydrogen bonds observed in the X-ray structure. This movement pulls the isocoumarin benzoyl carbonyl oxygen atom out of the oxyanion hole and displaces the active site Ser and His residues. The resulting geometry is quite unfavorable for a deacylation reaction. In addition to the displacements of the catalytic residues, the 7-substituent can electronically deactivate the isocoumarin benzoyl carbonyl toward deacylation and the ortho substituent can sterically hinder the approach of a solvent nucleophile to the benzoyl carbonyl group. Similar arguments have been used to explain the stability of other acyl enzymes including carbamoylchymotrypsin (Robillard et al., 1972), indolylacryloylchymotrypsin (Henderson 1970), azapeptide derivatives of the serine proteases (Gupton et al., 1984), and two benzoxazinone complexes of PPE (Radhakrishnan et al., 1987). Thus, the stability of acyl enzymes formed upon reaction of serine protease by heterocyclic inactivators is determined by several factors, only one of which is reaction with His-57. At present, the only crystal structure that contains His-57 and Ser-195 covalent bond formation with an inactivator is a complex of PPE inhibited by a β-lactam inhibitor (Navia et al., 1987). We will report additional examples in future papers.

Summary. The structure of the acyl enzyme formed upon inhibition of PPE by 4-chloro-3-ethoxy-7-guanidinoisocoumarin has been determined to near-atomic resolution. In addition to an ester bond linking the inhibitor to Ser-195, the 7-guanidino group forms hydrogen bonds with the carbonyl oxygen atom and the hydroxyl oxygen atom of Thr-41. Molecular modeling of the acyl enzyme structure and a proposed Michaelis complex allowed us to improve the inhibitory potency of the isocoumarin PPE inactivators by 2–9-fold relative to 7-amino-4-chloro-3-ethoxyisocoumarin. As predicted, *t*-BuHNCO-EIC and PhCSNH-EIC ($k_{obs}/[I]$ = 8100 M^{-1} s^{-1} and 12000 M^{-1} s^{-1}) were the best inhibitors discovered in this study and are among the best PPE inhibitors reported in the literature. Furthermore, the acyl enzyme derived from *t*-BuHNCO-EIC is extremely stable ($t_{1/2}$ for deacylation > 48 h). Other reported PPE inhibitors have inactivation rates below 2500 M^{-1} s^{-1}, with the exception of 2-ethoxybenzoxazin-4-one [5000 M^{-1} s^{-1}, recalculated from Hedstrom et al. (1984)] and 4-chloro-3-methoxy-7-[(*N*-tosylphenylalanyl)amino]isocoumarin with $k_{obs}/[I]$ = 6500 M^{-1} s^{-1} (Harper & Powers, 1985). However, in both these cases the acyl enzyme complexes are unstable and the enzyme regained full activity within a few hours.

A limited number of enzyme–small molecule complexes have been determined crystallographically, and at present it

is difficult to predict with confidence the exact binding mode of a new heterocyclic inhibitor structure to the active site of a serine protease. Structural results with two different isocoumarin inhibitors indicate that relatively small differences in the inhibitor can result in significantly different binding modes to the enzyme. It is clear that the crystal structures of many additional enzyme–inhibitor complexes, of similar inhibitors bound to both the same enzyme and structurally homologous enzymes, must be determined before we know the rules that determine the binding of small molecules to enzymes.

References

Bieth, J., Spiess, B., & Wermuth, C. G. (1974) *Biochem. Med. 11*, 350–357.

Bode, W., Wei, A.-Z., Huber, R., Meyer, E. F., Travis, J., & Neumann, S. (1986) *EMBO J. 5*, 2453–2458.

Bode, W., Meyer, E., & Powers, J. C. (1989) *Biochemistry 28*, 1951–1963.

Deisenhofer, J., Remington, S. J., & Steigemann, W. (1985) *Methods Enzymol. 115B*, 303–323.

Dunitz, J. D. (1979) in *X-ray Analysis and the Structure of Organic Molecules*, pp 366–384, Cornell University Press, Ithaca, NY.

Erlanger, B. F., Kokowsky, N., & Cohen, W. (1961) *Arch. Biochem. Biophys. 95*, 271–278.

Gund, P., Halgren, T. A., & Smith, G. M. (1987) *Annu. Rep. Med. Chem. 22*, 269–279.

Gupton, B. F., Carrol, D. L., Tuhy, P. M., Kam, C. M., & Powers, J. C. (1984) *J. Biol. Chem. 259*, 4279–4287.

Harper, J. W., & Powers, J. C. (1985) *Biochemistry 24*, 7200–7213.

Hedstrom, L., Moorman, A. R., Dobbs, J., & Abeles, R. H. (1984) *Biochemistry 23*, 1753–1759.

Henderson, R. (1970) *J. Mol. Biol. 54*, 341–354.

Jack, A., & Levitt, M. (1978) *Acta Crystallogr. A34*, 931–935.

Janoff, A., & Dearing, R. (1980) *Am. Rev. Respir. Dis. 121*, 1025–1029.

Jones, T. A. (1978) *J. Appl. Crystallogr. 11*, 268–272.

Kam, C.-M., Fujikawa, K., & Powers, J. C. (1988) *Biochemistry 27*, 2547–2557.

Kitz, R., & Wilson, I. B. (1962) *J. Biol. Chem. 237*, 3245–3249.

Luzatti, V. (1952) *Acta Crystallogr. 5*, 802–810.

Meyer, E. F., Presta, L. G., & Radhakrishnan, R. (1985) *J. Am. Chem. Soc. 107*, 4091–4093.

Meyer, E. F., Cole, G., Radhakrishnan, R., & Epp, O. (1988a) *Acta Crystallogr. B44*, 26–38.

Meyer, E. F., Clore, G. M., Gronenborn, A. M., & Hansen, H. A. S. (1988b) *Biochemistry 27*, 725–730.

Mido, Y., Fujta, F., Matsuura, H., & Machida, K. (1981) *Spectrochim. Acta 37A*, 103–112.

Navia, M. A., Springer, J. P., Lin, T.-Y., Williams, H. R., Firestone, R. A., Pisano, J. M., Doherty, J. B., Finke, P. E., & Hoogsteen, K. (1987) *Nature (London) 327*, 79–82.

Navia, M. A., McKeever, B. M., Springer, J. P., Lin, T.-Y., Williams, H. R., Fluder, E. M., Dorn, C. D., & Hoogsteen, K. (1989) *Proc. Natl. Acad. Sci. U.S.A. 86*, 7–11.

Powers, J. C., & Bengali, Z. H. (1986) *Am. Rev. Respir. Dis. 134*, 1097–1100.

Powers, J. C., & Harper, J. W. (1986) in *Proteinase Inhibitors* (Barrett, A. J., & Salvensen, G., Eds.) pp 55–152, Elsevier, Amsterdam.

Radhakrishnan, R., Presta, L. G., Meyer, E. F., & Wildonger, R. (1987) *J. Mol. Biol. 198*, 417–424.

Robillard, G. T., Powers, J. C., & Wilcox, P. E. (1972) *Biochemistry 11*, 1773–1784.

Schechter, I., & Berger, A. (1967) *Biochem. Biophys. Res. Commun. 27*, 157–162.

Schwager, P., Bartels, K., & Jones, A. (1975) *J. Appl. Crystallogr. 8*, 275–280.

Schweitzer, W. B., & Dunitz, J. D. (1982) *Helv. Chim. Acta 65*, 1547–1554.

Steigemann, W. (1974) Ph.D. Dissertation, T. U. Muenchen.

Sudha, L. V., & Sathyanarayana, D. H. (1984) *J. Mol. Struct. 125*, 89–96.

Swanson, S. M. (1988) *Acta Crystallogr. A44*, 437–442.

Takahashi, L. H., Radhakrishnan, R., Rosenfield, R. E., Meyer, E. F., Trainor, D. A., & Stein, M. (1988) *J. Mol. Biol. 201*, 423–428.

Takahashi, L. H., Radhakrishnan, R., Rosenfield, R. E., Meyer, E. F., & Trainor, D. A. (1989) *J. Am. Chem. Soc. 11*, 3368–3374.

Vassilev, G. (1982) *J. Mol. Struct. 82*, 35–41.

Wei, A.-Z., Mayr, I., & Bode, W. (1988) *FEBS Let. 234*, 367–373.